Geosci. Model Dev. Discuss., 5, 1435–1481, 2012
www.geosci-model-dev-discuss.net/5/1435/2012/
doi:10.5194/gmdd-5-1435-2012

Geoscientific
Model Development
Discussions

Development of high resolution land surface parameters for the Community Land Model

Y. Ke, L. R. Leung, M. Huang, A. M. Coleman, H. Li, and M. S. Wigmosta

Pacific Northwest National Laboratory, Richland WA, USA

Received: 3 April 2012 – Accepted: 25 April 2012 – Published: 12 June 2012

Correspondence to: Y. Ke (yinghai.ke@pnnl.gov)

Published by Copernicus Publications on behalf of the European Geosciences Union.

Abstract

There is a growing need for high-resolution land surface parameters as land surface models are being applied at increasingly higher spatial resolution offline as well as in regional and global models. The default land surface parameters for the most recent version of the Community Land Model (i.e. CLM 4.0) are at 0.5° or coarser resolutions, released with the model from the National Center for Atmospheric Research (NCAR). Plant Functional Types (PFTs), vegetation properties such as Leaf Area Index (LAI), Stem Area Index (SAI), and non-vegetated land covers were developed using remotely-sensed datasets retrieved in late 1990's and the beginning of this century. In this study, we developed new land surface parameters for CLM 4.0, specifically PFTs, LAI, SAI and non-vegetated land cover composition, at 0.05° resolution globally based on the most recent MODIS land cover and improved MODIS LAI products. Compared to the current CLM 4.0 parameters, the new parameters produced a decreased coverage by bare soil and trees, but an increased coverage by shrub, grass, and cropland. The new parameters result in a decrease in global seasonal LAI, with the biggest decrease in boreal forests; however, the new parameters also show a large increase in LAI in tropical forest. Differences between the new and the current parameters are mainly caused by changes in the sources of remotely sensed data and the representation of land cover in the source data. The new high-resolution land surface parameters have been used in a coupled land-atmosphere model (WRF-CLM) applied to the western US to demonstrate their use in high-resolution modeling. Future work will include global offline CLMsimulations to examine the impacts of source data resolution and subsequent land parameter changes on simulated land surface processes.

1 Introduction

As the terrestrial component of earth system models, land models simulate land surface processes that control the exchanges of water, energy and momentum between soil, vegetation and atmosphere. The Community Land Model (CLM) is a land model within the Community Earth System Model (CESM), formerly known as Community Climate System Model (CCSM) (Oleson et al., 2010). It was designed for coupling with atmospheric models such as Community Atmosphere Model (CAM), and provides estimation of surface albedos, upward longwave radiation, sensible heat flux, latent heat flux, water vapor flux and surface CO_2 exchanges required by atmospheric models (Oleson et al., 2010). The land surface parameters in CLM are represented with a nested subgrid hierarchy in which spatial heterogeneity of the land surface is considered for each model grid. Grid cells are composed of a different number of land units including glacier, lake, wetland, urban and vegetated surfaces. Vegetated surfaces are represented with composition of 15 possible Plant Functional Types (PFTs) plus bare ground. For vegetation characteristics, leaf and stem area indices and canopy top and bottom height parameters are described for each PFT. Soil color, soil texture and soil organic matter density, in addition to a number of urban parameters, are required for ground surface parameters.

CLM has been widely applied at continental and global scales to understand how land processes and anthropogenic impact on land states affect climate and spatiotemporal change of the climate (e.g., Bonan et al., 2002b; Dickinson et al., 2006). In continental or global studies, CLM typically operates over a coarse spatial resolution (e.g., 1° by 1° or bigger grid cells). Recent studies have emerged to apply CLM at the regional scale and even at the small watershed scale (Li et al., 2011). CLM has also been used in an initial effort as the land surface component of a regional earth system model based on the Weather Research and Forecasting (WRF) model (Leung et al., 2006). Regional and sub-regional applications require CLM to run at much finer spatial resolution (e.g., 1–20 km grid cells) in order to better represent the effects of land surface heterogeneity and provide climate information at the scales needed for impact assessment (Leung et al., 2006). These requirements demand land surface parameters to be provided at a resolution similar to or finer than that of the model. In the current version of CLM (CLM 4.0) the land surface parameters are provided at 0.5° by 0.5° or coarser resolutions. For example, lake and wetland data were derived from Cogley's (1991) 1° by 1° data for perennial freshwater lakes and swamps/marshes; PFT Leaf Area Index (LAI) were derived from Moderate Resolution Imaging Spectroradiometer (MODIS) satellite data and were aggregated to a 0.5° resolution. There are limitations in using these surface datasets to support regional-scale modeling.

In addition to the coarse spatial resolution, the CLM 4.0 land surface parameters were generated using temporally mixed, somewhat outdated, and in some cases, not fully validated data sources. For example, the lake and wetland data was sourced from Global Hydrographic Data in 1991 (Cogley, 1991); PFTs fractional cover data was derived using a combination of the 2001 MODIS Vegetation Continuous Field (VCF), MODIS land cover product with unknown year (Lawrence and Chase, 2006, 2007), and 1992–1993 AVHRR Continuous Field Tree Cover Project data (Lawrence and Chase, 2007; Lawrence et al., 2011); the MODIS VCF dataset, which contains proportional estimates of bare soil, trees and herbaceous vegetation in each pixel area, has not been extensively validated, especially for the estimates of bare soil and herbaceous cover (Hansen et al., 2003; Jeganathan et al., 2009; Montesano et al., 2009).

In recent years, substantial effort has been made in developing improved characterizations of global land cover and vegetation based on MODIS imagery, or other available satellite sensor products, in order to provide accurate and continuous land parameters for land surface and climate modeling. The MODIS Collection 5 Land Cover Type (MCD12Q1 C5) product became available in 2008 to provide an update of the Collection 4 product (MOD12Q1 C4) (Friedl et al., 2010). This dataset consists of five different land cover classifications including the 17-class International Geosphere-Biosphere Programme (IGBP) classification (Loveland and Belward, 1997) and a 12-class PFT classification produced for each year from 2000 to present at 500 m resolution (Friedl et al., 2010). Compared to MOD12Q1 C4, the C5 product yields significant improvements in both spatial resolution (500 m for C5 and 1000 m for C4 data) and classification accuracy (Friedl et al., 2010). The MODIS LAI product is also available as an 8-day composite at 1000 m resolution and has been widely used in land surface models. However, due to the presence of clouds, snow cover, and instrument problems, the MODIS LAI product produced considerable noise and gaps. To reduce the noise, the current CLM 4.0 PFT LAI parameters were derived by averaging high-quality MODIS LAI data during 2001–2003 onto coarser resolution (0.5°) grid cells, and partitioning the averaged LAI for each PFT. Yuan et al. (2011) presented a re-processed global MODIS LAI product from years 2000 to 2010 using a temporal spatial filter algorithm to improve the LAI data quality while preserving the spatial resolution. Compared to the current MODIS LAI data, it significantly removed unrealistic fluctuations and provided more accurate, spatiotemporally continuous and consistent LAI values. This improved LAI product is currently the most spatially and temporally complete LAI data that has been fully validated. With the most recent updated and improved land cover and vegetation products, it is feasible to regenerate land surface parameters for CLM 4.0 – with higher resolution and better accuracy.

This study aims to develop new high-resolution global CLM 4.0 land surface parameters based on the best available MODIS land surface data, and presents an example application of the new parameters in regional modeling using the Weather Research and Forecasting (WRF) coupled with CLM (WRF-CLM) over the western US at 12 km resolution. Specifically, the new parameters generated include percentage of lake, wetland, urban and glacier, PFT fractional cover, and monthly PFT LAI and SAI, all at 0.05° resolution. New parameters were compared against the current CLM 4.0 parameters globally and regionally, and the PFTs were further evaluated over the conterminous US (CONUS) domain using the 2006 National Land Cover Database (NLCD) data (http://www.mrlc.gov/) and the United States Department of Agriculture National Agriculture Statistics Service (USDA NASS) statistical report on US crop area (http://www.nass.usda.gov/).

2 Method

The source data that was used to generate the new high-resolution land surface parameters in comparison with the CLM 4.0 land surface parameters is presented in Table 1. The method of data development is described in the following sections.

2.1 New Plant Functional Types mapping

The MCD12Q1 C5 PFT classifications for the year 2005 were directly used to determine seven PFTs including Needleleaf Evergreen trees, Needleleaf Deciduous trees, Broadleaf Evergreen trees, Broadleaf Deciduous trees, shrub, grass and crop for each 500 m pixel. The WorldClim 5 arc-min (0.0833°) (Hijmans et al., 2005) climatological global monthly surface air temperature and precipitation data was interpolated to 500 m grids and used to further reclassify the 7 PFTs into 15 PFTs in the tropical, temperate and boreal climate groups based on climate rules described by Bonan et al. (2002a). Similar to Lawrence and Chase (2007), fractions of C3 and C4 grasses were mapped based on the method presented in Still et al. (2003). Pixels with barren land and urban areas were reassigned to the bare soil class. The bare soil and the 15 PFTs in the 500 m grids were then aggregated to 0.05° grids and the fractional cover of each PFT was calculated.

2.2 New LAI and SAI mapping

The new PFT LAI mapping was based on the improved MODIS LAI 8-day composite product reprocessed by Yuan et al. (2011) and the 15-PFT classification described above. First, the 1-km 8-day improved MODIS LAI for the year 2005 was used to calculate a mean monthly LAI that was then interpolated to a set of 500 m grids using Nearest Neighbour sampling method. Combined with the 15 PFTs resulted from the reclassification of the MCD12Q1 C5 product at a 500 m resolution, monthly LAI values for each PFT was determined. Finally, the PFT LAI was calculated by averaging LAIs for each PFT within the 0.05° grids. It has been widely recognized that MODIS often underestimates LAI during the winter season at high latitudes (e.g., latitude >60° N) because of snow cover and low sun angles. To account for the underestimation, the evergreen phenology correction was performed following Lawrence and Chase (2007) so that LAI values of evergreen PFTs were only allowed to reach a minimum fraction of the annual maximum PFT LAI from the MODIS improved LAI product. The maximum PFT LAI value listed in Bonan et al. (2002a) was used to constrain the range of PFT LAIs. Monthly PFT SAI values were calculated following the same method described in Lawrence and Chase (2007) using the monthly PFT LAI values, the PFT percentage, and minimum PFT SAI values.

2.3 Non-vegetated land cover mapping

The distribution of global lakes was derived from the MCD12Q1 C5 IGBP classification of water bodies using the ESRI Data and Maps landmass boundaries (www.esri.com) to constrain water bodies to inland water only. The distribution of wetlands was derived from the MCD12Q1 IGBP classification of permanent wetlands, glacier from classification of snow and ice, and urban from classification of urban and built-up areas. All 500 m pixels were aggregated to 0.05° grid cells to generate the fractional cover of lake, wetland, glacier and urban.

2.4 New parameter mapping evaluation

The new land surface parameters including PFTs and non-vegetated land fractional cover were compared against the CLM 4.0 land surface parameters over the global land area and three specific regions: Boreal (50° N$\sim$70° N), Amazon (80° W$\sim$30° W, 20° S$\sim$10° N), and Sahara and Arabia (20° W–60° E, 15° N–35° N). The new PFT and non-vegetated land parameters at 0.05° resolution were aggregated to 0.5° grids to be comparable with the current CLM 4.0 parameters. Global maps of the new and CLM 4.0 land surface parameters were generated to demonstrate the spatial similarities and differences between the two sets of parameters. Overall average values of percentage of PFTs and non-vegetated land cover were also compared with the current CLM 4.0 parameters globally and regionally. The number of PFTs per grid of both the new and current CLM 4.0 parameters were mapped and compared in order to evaluate the effect of the higher resolution in the new parameters.

To further assess the accuracies of PFTs, PFTs from both the new and CLM 4.0 land parameters were compared with the 2006 NLCD and the 2007 NASS crop statistical data over CONUS. The 2006 NLCD is a 16-class land cover data over CONUS at a spatial resolution of 30 m which was produced primarily on the classification of Landsat Enhanced Thematic Mapper+(ETM+) circa 2006 satellite data (Fry et al., 2011). The USDA NASS provides agriculture statistics every five years for US states and counties, and include crop type, crop area, production, etc. (http://www.nass.usda.gov/). Considering the difference in the CLM PFT and NLCD classification scheme, the land cover classes in the new PFT parameters, CLM 4.0 PFT parameters and the NLCD were reclassified into five general land cover types, i.e., bare soil, trees, shrub, grass, and crops, based on the recoding method in Table 2. Because the "bare" class in the CLM PFT parameters was defined as any non-vegetated area including bare land and open water, the open water areas were eliminated from the "bare" parameter using the new and CLM 4.0 lake percentage parameter respectively for the new PFT parameters and CLM 4.0 PFT parameters. The reclassified NLCD 30m land cover was re-projected then aggregated to a 0.5° grid resolution. The percentages of bare soil, trees, shrub, grass and cropland were calculated for each 0.5° grid and then compared with the new and CLM 4.0 PFT parameters over CONUS. In our study the report on total non-woody crop acreage in the year 2007 was used to provide a reference crop area for comparison with the new and CLM 4.0 estimated cropland over the US

Seasonal average LAI and SAI were calculated by combining the composition of PFTs and monthly PFT LAI and SAI for both the new and current CLM 4.0 parameters. Spatial and statistical comparison of LAI and SAI from both parameter sets over global and regional land areas was performed. In addition, LAI values were also evaluated against the MODIS improved LAI product at the global extent. Monthly PFT LAIs were calculated for the new and current CLM 4.0 parameters by averaging LAI values for each PFT across the Northern and Southern Hemisphere respectively. Plots of monthly PFT LAIs were used to assess the seasonal cycles of individual PFT LAI.

2.5 Regional climate simulation

CLM has been used as the land surface model in the CCSM for global climate modeling since CCSM 1.0 was developed in the mid-1990s. CLM has also been coupled to the WRF model (Skamarock et al., 2008) to simulate the regional climate of the western US (Leung et al., 2006; Jin et al., 2010; Subin et al., 2011). In the previous implementation of WRF-CLM, CLM was coupled to WRF through a subroutine call from WRF to CLM as one of a few options for land surface modeling. Because the CLM surface parameters were only available at 0.5° resolution, Subin et al. (2011) used various land surface datasets developed for WRF to prescribe surface parameters for WRF-CLM. For example, they used a fixed mapping from WRF's 24 US Geological Survey (USGS) land-use categories to groups of up to 4 of CLM's 17 PFTs. Monthly LAI was prescribed for each PFT, so LAI varied with PFT but not geographically. These approaches did not take advantage of more detailed surface data normally prescribed in CLM for modeling biophysical processes.

More recently, through the development of the Regional Arctic Climate System Model (RACM) (Maslowski et al., 2011), WRF has been implemented as part of CCSM to make use of the CCSM flux coupler for coupling earth system components. Using RACM, we have coupled WRF with CLM using the flux coupler for exchange of surface fluxes and atmospheric and land surface states. A simulation has been configured for the western US at a 12 km grid resolution. To take full advantage of the high-resolution domain, the new 0.05° resolution CLM surface parameters described above were used to specify non-vegetated land cover, PFTs, LAI, and SAI. Soil texture were obtained from the WRF 1 km resolution soil data derived from STATSGO. Other surface data including soil color and soil organic matter were derived from CLM 4.0 default data provided by NCAR (http://www.cesm.ucar.edu/models/cesm1.0/clm/).

Since the western US WRF domain was defined using a Lambert Conformal projection with a fixed distance of 12 km between neighboring grid cells, the model grids were shape-distorted when projected to a regular latitude-longitude geographic coordinate system, which is used by the CLM land surface data. Although the existing WRF Preprocessing System (WPS) provides several interpolation options such as nearest neighbor, four-point bilinear, four-point simple or weighted average, the WPS is not designed to generate land surface data for CLM. Moreover, the WPS interpolation methods are not accurate, especially for continuous fractional data. In this study, we developed an interpolation method to map the 0.05° CLM land surface data onto the WRF model grids based on an area-weighted average approach. For each WRF model grid, the method initially finds the intersecting CLM grids by determining whether one or more corners of a CLM grid are inside the WRF model grid. Next, each of the intersecting CLM grids is divided into 100 × 100 subgrids with a regular latitude/longitude interval. The total area of the subgrid whose center point is inside the WRF model grid is calculated and its proportion to the WRF model grid area is used as a weight for the intersecting CLM grid. The weighted average of all intersecting CLM grid attributes (e.g., fractional land cover, PFTs, LAI, etc.) is assigned to the WRF model grid.

A one-year simulation was performed from 1 October 2003 – 30 September 2004, with WRF initial and lateral boundary conditions obtained from the North American Regional Reanalysis (NARR) at a 32 km grid resolution (http://www.emc.ncep.noaa.gov/mmb/rreanl/). The NARR soil moisture and temperature at 0Z on 1 October 2003 was re-gridded to the WRF grid bi-linearly using the WPS, and vertically interpolated linearly to obtain CLM soil moisture and temperature profiles for model initialization.

3 Results

From Table 1, all new parameters have a much higher spatial resolution than the current CLM 4.0 land surface parameters. It is clear that the new parameters were consistently derived from the latest release of the MODIS land cover product MCD12Q1 C5, while the current CLM 4.0 parameters were derived from various data sources. In addition, the newly developed parameters represent consistent land surface characteristics for 2005 while the source data of the current CLM 4.0 parameters were derived from information that spans across 1991 to 2008 with no internal consistency.

3.1 New Plant Functional Type parameters

Table 3 and Fig. 1 illustrate the spatial and statistical differences between the new and CLM 4.0 PFT parameters. Bare soil dominates the global land coverage. However, there is a large difference in bare soil between the two datasets. For the new parameters, the bare soil percentage decreased to 24.7 % from 33.5 % found in the CLM 4.0 parameters (Table 3); areas of change are found mainly in the high latitude areas of North America, western US, South Africa and central Australia, where the new parameters showed significantly increased percentage of shrub coverage over bare soil (Fig. 1a, b, Fig. 2a, b).

Figure 1c and d show similar spatial distribution of needleleaf trees in the new and CLM 4.0 PFT parameters, except that there is greater coverage in southeast US and far eastern Russia in CLM 4.0. Globally, both Needleleaf Evergreen Temperate trees and Needleleaf Evergreen Boreal trees have decreased coverage in the new parameters compared to CLM 4.0 (2.2 % compared to 3.0 %, 5.2 % compared to 6.4 %, respectively), but the Needleleaf Deciduous Boreal trees have increased coverage (2.3 % compared to 1.0 %). Regional statistics show that the differences are mainly in the boreal region, which has substantially lower coverage of Needleleaf Evergreen Boreal trees (21.0 % compared to 29.0 %) but greater coverage of Needleleaf Deciduous Boreal trees (10.6 % compared to 4.9 %) and Needleleaf Evergreen Temperate trees (4.0 % compared to 2.7 %). Interestingly, in the Amazon region, there are 0.4 % Needleleaf Evergreen Temperate trees in the new data that are not found in the CLM 4.0 parameters. No needleleaf trees were found in the Sahara & Arabia region for either set of parameters.

Broadleaf Evergreen trees are mostly distributed in the Amazon rainforest, central Africa and Southeast Asia in both the new and CLM 4.0 PFT parameters. From Fig. 1e and f, the new parameters have increased coverage in the areas of southern China, Europe and western Russia, where no significant amount (less than 1 %) of Broadleaf Evergreen trees are found in CLM 4.0 parameters. Across all lands, both Broadleaf Evergreen Tropical trees and Broadleaf Evergreen Temperate trees have an increased percentage in the new parameters (9.4 % compared to 8.7 % and 1.6 % compared to 1.4 %, respectively). The Amazon region had increased Broadleaf Evergreen Tropical trees (52.3 % compared to 49.8 %) but decreased Broadleaf Evergreen Temperate trees (1.1 % compared to 1.7 %). The Boreal region had 0.4 % of Broadleaf Evergreen Temperate trees in the new parameters while no such trees are found in CLM 4.0 parameters.

Figure 1g and h shows that the new parameters produced less spatial coverage of Broadleaf Deciduous trees than the current CLM 4.0 parameters, with a lower percentage across all land in Broadleaf Deciduous Tropical trees (2.8 % compared to 5.1 %), Broadleaf Deciduous Temperate trees (2.5 % compared to 3.3 %), and Broadleaf Deciduous Boreal trees (0.9 % compared to 1.2 %). Regional analysis showed that the Amazon region has a large decrease of Broadleaf Deciduous Tropical trees (5.8 % compared to 14.4 %) and a small decrease of Broadleaf Deciduous Temperate trees (0.1 % compared to 0.2 %). The Boreal region has a large decrease in Broadleaf Deciduous Boreal trees (2.4 % compared to 3.9 %).

Large differences are found in shrub coverage between the new and CLM 4.0 parameters (Fig. 2a, b). The new parameters produced a large concentrated distribution of shrub at the high latitude areas of North America, Mexico, South Africa and Australia, while the CLM 4.0 parameters show much less shrub percentage over these same areas. Globally, the new parameters have a large increase of Broadleaf Deciduous Temperate shrubs (11.2 % compared to 3.8 %), Broadleaf Evergreen Temperate shrubs (0.7 % compared to 0.1 %) and Broadleaf Deciduous Boreal shrubs (6.7 % compared to 5.4 %). In the Amazon region there is a large increase of Broadleaf Deciduous Temperate shrubs (6.5 % compared to 2.3 %) and a decrease of Broadleaf Deciduous Boreal shrubs (0.5 % compared to 1.0 %). The Boreal region has a large increase of Broadleaf Deciduous Boreal shrubs (39.3 % compared to 24.0 %) and an increase of Broadleaf Evergreen Temperate (0.3 % compared to 0 %) and Broadleaf Deciduous Temperate shrubs (0.3 % compared to 0.1 %). The Sahara & Arabia region has a large increase of Broadleaf Deciduous Temperate shrubs (9.9 % compared to 1.7 %), and an increase of Broadleaf Evergreen Temperate shrubs (0.6 % compared to 0 %).

Global distribution of grass shows less coverage of C3 grass in the new parameters at the high latitude areas, US Great Plains, and South Africa, but shows greater concentration in the Northwest US and around the fringes of Great Tibet (Fig. 2c, d). The distribution pattern of C4 grass is similar between the new and CLM 4.0 parameters, except there is an increased concentration of C4 grass in Brazil, Sahel, southern Africa and northern Australia. Globally, the new parameters have a small increase of C3 Arctic grass (3.1 % compared to 2.9 %), a decrease of C3 non-Arctic grass (6.7 % compared to 8.2 %), and a small increase of C4 grass (8.6 % compared to 7.5 %). In the Amazon region there is a decrease of C3 non-Arctic grass (3.0 % compared to 5.9 %) and an increase of C4 grass (22.1 % compared to 17.1 %). In the Boreal region, both C3 Arctic and non-Arctic grass have decreased contribution (9.1 % compared to 9.9 % and 4.1 % compared to 4.8 %), and C4 grass has a small increased contribution (0.1 % compared to 0 %). The Sahara & Arabia region has a decrease of C3 grass (0.4 % compared to 1.2 %), but a large increase of C4 grass (8.6 % compared to 5.8 %).

Across the globe, a considerable increase of cropland is reported in the new parameters (11.1 % compared to 8.5 %). The global distribution shows that the new parameters have a greater concentration of crop in the Midwest US, Europe, India and eastern China, but less crop coverage in eastern Africa. Regional analysis shows that the new parameters have a relatively large increase of crop in the Amazon (4.5 % compared to 3.0 %) and Boreal (10.2 % compared to 7.0 %), and a large decrease of crop in the Sahara & Arabia (1.8 % compared to 2.9 %).

Figure 3a, b shows the distribution of the number of PFTs within each 0.5°×0.5° grid cell for the new and CLM 4.0 parameters. The new parameters generally produce more PFT classes per grid or larger subgrid variability of PFTs, especially in temperate climate such as the eastern US, Europe, and eastern China. However, the new parameters have a lower number of PFTs in the higher latitude areas of the Northern Hemisphere (> 60° N) and semi-arid areas such Western Australia, where shrub dominates in the new parameters while CLM 4.0 indicates a mix of shrub and bare soil. The latitudinal distribution of the average number of PFTs shows a similar pattern in the two datasets (Fig. 3c). Both parameters have high vegetation abundance at the mid-latitude zones (40° N~60° N, 40° S~60° S), and low vegetation abundance at high latitude zones (60° N~90° N, 60° S~90° S). In the low to mid-latitude zone (40° N~40° S), both the new and CLM 4.0 parameters have a decreasing number of PFTs around the equator, 20° N, and 30° S, and an increasing number of PFTs around 10° N and 10° S. Except between 15° S and 35° S, the new parameters produced more average PFTs classes in each grid than the CLM 4.0 parameters across all latitudes.

3.2 Evaluation of Plant Functional Type parameters over CONUS

From the analyses discussed above, the US is one of the regions where large differences are found in the spatial distribution of PFTs between the two datasets. To assess the relative merits of the datasets, PFT parameters from the new and CLM 4.0 datasets are evaluated using the 2006 NLCD data. Figure 4 shows the spatial patterns of land cover classes from the new, CLM 4.0, and NLCD parameters. Bare soil in NLCD data is mainly concentrated in the arid regions of western US, with some coverage scattered in other parts of US (Fig. 4c). The new PFT parameters show a similar spatial pattern (Fig. 4a), but CLM 4.0 significantly overestimates bare soil coverage in the midwestern and western US and has a much lower contribution in the eastern US Over

CONUS, the area covered by bare soil represented by CLM 4.0 is considerably higher than both the new PFT and NLCD parameters (14.8 % compared to 2.7 % in new PFT parameters and 2.0 % in NLCD).

The spatial coverage of trees is similar between CLM 4.0 and NLCD, with CLM 4.0 slightly overestimating trees over CONUS (31.5 % compared to 28.8 %). The new parameters have similar spatial distribution of trees in eastern and northwestern US, but they have much less coverage in the Midwestern US, which led to an overall underestimation of tree percentage over CONUS (25.2 % compared to 28.8 %). Shrub distribution is similar between the new PFT parameters and NLCD data: shrubs are mainly concentrated in the southwestern US, with some coverage in the southeastern US; however, shrubs in CLM 4.0 are limited to the western US with much lower coverage, and no shrub (<1 %) cover found in the east. These result in a large underestimation of shrubs over CONUS in CLM 4.0 (4.8 % compared to 21.4 %). The underestimation has been significantly alleviated in the new parameters.

Over CONUS, the new parameters have a relatively accurate estimation of grassland area (28.3 % compared to 28.5 %), while the current CLM 4.0 parameters have a slight underestimation (25.1 % compared to 28.5 %). However, the spatial distribution of grassland is very different between the new PFT parameters and the NLCD data. While both CLM 4.0 and NLCD have grassland distributed across CONUS, the new parameters have grassland concentrated in the West with little coverage in the northern Great Plains, Midwest, and eastern US Instead, the latter regions have a larger coverage of crop in the new parameters, as shown in Fig. 4m, n and o. Over CONUS, both the new and CLM 4.0 parameters overestimate crop contribution compared to NLCD (25.0 % in new parameters and 20.5 % in CLM parameters compared to 15.5 % in NLCD). However, it is likely that NLCD underestimates crop coverage since the NASS survey shows that a crop area of 20.3 % in 2007 and 21.5 % in 2002 over CONUS (Table 4).

3.3 New LAI and SAI parameters

Across all land, Table 5 shows that the new parameters have large decreases in combined LAI for all seasons, with the largest decrease in the months of JJA (0.93 compared to 1.09) and the smallest decrease in the months of DJF (0.6 compared to 0.68). Figure 5 shows that the decreases are mainly distributed over the high latitude areas of the Northern Hemisphere, which is covered mostly by boreal needleleaf trees, and the eastern US that is covered by mixed trees, grass and crops in the new parameters and CLM 4.0 parameters. Regional analysis (Table 5) shows that the Northern Hemisphere boreal region has large decreases in LAI in all seasons, with the largest decrease in the summer (1.46 compared to 1.97) and smaller decrease in the other seasons (0.52 compared to 0.75 in winter, 1.1 compared to 1.34 in spring, and 0.61 compared to 0.83 in the autumn).

In contrast, the Amazon region has considerably higher LAI in all seasons in the new parameters (Fig. 5 and Table 5), with the largest increase during the summer season (3.49 compared to 3.09) and the smallest increase in the spring season (3.38 compared to 3.22). The Central Africa and South Asia tropical forests also have a higher LAI during all seasons in the new parameters (Fig. 5). Sahara & Arabia regions have similar LAI during all seasons. In the south-central region of Africa where land cover is dominated by broadleaf deciduous trees, shrub and grass, the new parameters have increased LAI during austral spring and summer (Fig. 5a, d), and decreased LAI during austral autumn and winter (Fig. 5b, c).

Evaluation of the new parameters against the MODIS improved LAI product (Fig. 6) shows that in the summer season, there are no observable differences in most land areas except for the slightly lower LAI in the eastern US and western Europe and higher LAI in coastal central Africa and Burma. In the months of MAM, SON, and DJF, the new parameters have distinctly higher LAI than the MODIS improved LAI observations in the Amazon, Central Africa and Southeast Asia, which are covered by evergreen tropical forests, and the high latitude areas in the Northern Hemisphere, which includes Evergreen Boreal forest of northern North America, Europe and Russia.

Since SAI parameters are calculated from LAI following the same method in Chase and Lawrence (2007), it is not surprising that the new parameters have decreased SAI over all land during all seasons. Regional analysis shows that the boreal region has large decrease in SAI, with the largest decrease in boreal autumn (0.55 compared to 0.80). The Amazon region has a small reduction in the months MAM and SON for SAI, but decreased SAI for other seasons. The Sahara & Arabia region has increased SAI for all seasons. Spatial distribution of the differences shows a similar pattern with LAI differences (Fig. 7). Throughout the year, the new parameters have increased SAI over the Amazon tropical forests, but decreased SAI over high latitude Northern Hemisphere boreal forest, and eastern US The African Savannah area has a slightly decreased DJF SAI, but slightly increased SON SAI.

3.4 New PFT LAI Parameters in Northern and Southern Hemisphere

The phenology cycles of each PFT LAI in the Northern and Southern Hemisphere are shown in Figs. 8 and 9, respectively. Overall there are reasonable agreements between the two datasets, showing a larger phenology cycle for needleleaf and broadleaf deciduous boreal trees and broadleaf deciduous temperate trees compared to other PFTs. In addition, seasonal variations in phenology are generally larger in the Northern Hemisphere than Southern Hemisphere and distinct shifts in the seasonal timing are also noticeable in the PFTs, corresponding to the dominance of land mass in the subtropical/mid-latitude versus tropical regions and the change of season in the two hemispheres.

In the Northern Hemisphere, both the new and CLM 4.0 parameters have similar seasonal LAI values and phenology for needleleaf evergreen temperate trees (Fig. 8a). For needleleaf evergreen boreal trees, both parameter sets have similar LAI cycle in terms of the growing season start and end month, but the new parameters have considerably decreased LAI values compared to the CLM 4.0 parameters (1.9 compared to 2.1). For needleleaf deciduous boreal trees, the new parameters have similar LAI values as the current CLM 4.0 parameters, but with an earlier and more symmetrical growing season.

Figure 8b shows that the Broadleaf Evergreen Tropical trees have slightly lower average LAI in the new parameters (3.8 compared to 4.2), and the Broadleaf Evergreen Temperate trees have a substantially lower LAI in the new parameters (3.1 compared to 3.8). There is no distinct seasonality for both Broadleaf Evergreen Tropical and Temperate trees in both sets of parameters.

Figure 8c shows that both sets of parameters have generally similar seasonal cycles for Northern Hemisphere broadleaf deciduous trees. For Broadleaf Deciduous Tropical trees, the new parameters have slightly higher maximum LAI values (2.8 compared to 2.6) and slightly lower minimum LAI values (1.4 compared to 1.6). For Broadleaf Deciduous Temperate trees, the new parameters have a longer growing season and more distinct seasonal fluctuation, with noticeably higher maximum LAI values (3.1 compared to 2.7) and slightly lower minimum LAI values (0.9 compared to 1.1). Similarly, the Broadleaf Deciduous Boreal trees also have more distinct seasonal fluctuation in the new parameters, with a substantially higher maximum LAI value (3.8 compared to 2.9). In addition, the new parameters result in an earlier growing season and more symmetric seasonal LAI phenology for the Broadleaf Deciduous Boreal trees.

Figure 8d shows that the new parameters have similar LAI seasonal phenology and magnitude for Broadleaf Deciduous Temperate shrubs. For Broadleaf Evergreen Temperate shrub, the new parameters generate similar LAI phenology yet slightly lower LAI values (mean LAI of 0.7 compared to 0.9). For Broadleaf Deciduous Boreal shrub, the new parameters also have similar LAI phenology but substantially lower PFT LAI throughout the year (mean LAI of 0.4 compared to 0.9).

Figure 8e shows that the new parameters have similar LAI phenology cycles for the Northern Hemisphere grass PFTs. For C4 grass, the new parameters also have similar LAI values as the CLM 4.0 parameters. For both C3 Arctic and C3 non-Arctic grass, the new parameters generate substantially lower LAI throughout the year, with a mean

LAI of 0.4 compared to 0.9 for C3 Arctic grass and 0.8 compared to 1.1 for C3 non-Arctic grass. For crops, Fig. 8f shows that the new parameters have generally similar phenology pattern but slightly greater seasonal fluctuation than CLM 4.0, with higher maximum LAI value (1.9 compared to 1.7) and lower minimum LAI value (0.6 compared to 0.8).

In the Southern Hemisphere, the new parameters have large differences in PFT LAI for Needleleaf trees (Fig. 9a). Both Needleleaf Evergreen Temperate trees and Needleleaf Evergreen Boreal trees have a substantially lower PFT LAI throughout the year in the new parameters, with a mean LAI value of 1.4 compared to 2.1 for the former PFT and mean LAI value of 0.9 compared to 2.4 for the latter. Neither PFT shows a significant phenology cycle in the new or CLM 4.0 parameters. No Needleleaf Deciduous Boreal trees are found in the Southern Hemisphere for the CLM 4.0 parameters, but the new parameters report a sparse coverage of Needleleaf Deciduous Boreal trees, with 4 % distributed in the Southern Hemisphere and 96 % distributed in the Northern Hemisphere. The Southern Hemisphere Needleleaf Deciduous Boreal trees have an average LAI of 1.0.

For Broadleaf Evergreen, Fig. 9b shows that the new and CLM 4.0 parameters have good agreement. For Broadleaf Deciduous, Fig. 9c shows that the new parameters have a significantly different PFT LAI phenology cycle for the Southern Hemisphere, with the maximum LAI occurring about two months earlier and with larger seasonal fluctuations than the CLM 4.0 parameters. Figure 9d shows that the new parameters generally have a lower LAI for Southern Hemisphere shrubs. For Broadleaf Evergreen Temperate shrubs, the new parameters also had a different phenology pattern, with the maximum LAI value in austral summer compared to September and October.

Figure 9e shows that the new parameters have lower PFT LAI values for Southern Hemisphere grasses. For C3 Arctic grass, the new parameters produced a similar phenology cycle, yet lower LAI values than the current CLM 4.0 parameters throughout the year, with average LAI values of 0.6 compared to 0.9 in CLM 4.0 parameters. For C3 non-Arctic grass, the new parameters show the LAI phenology cycle begins two months earlier, with maximum LAI in February compared to April, and slightly lower maximum LAI values (1.4 compared to 1.6). Similarly, for C4 grass, the new parameters also had an earlier (February compared to April) and slightly lower maximum LAI (1.6 compared to 1.8). Figure 9f shows that the new parameters have different LAI phenology for the Southern Hemisphere crops, with the new parameters peaking two months earlier than the CLM 4.0 parameters (February compared to April) with smaller seasonal fluctuation.

3.5 Non-vegetated parameters

Over all land, the new parameters have significantly increased coverage of lake compared to the current CLM 4.0 parameters (1.4 % compared to 0.52 %). Figure 10a, b shows that the large increases are mainly distributed in the regions of Canadian Shield, Scandinavia, Siberia, and Tibet plateau. The contribution from wetland also has distinct increase in the new parameters (1.0 % compared to 0.25 %). Likewise, the wetland areas represented in the new parameters are mainly distributed in Canadian Shield, Scandinavia, west Siberia regions, and south America and central Africa also have increased contribution from wetland (Fig. 10c, d).

The new parameters reduce urban area (0.44 % compared to 0.64 %) over all land, and Fig. 10e, f shows significant decrease over India and eastern China. There is a slight increase in urban area over the US and southeast Brazil. Glacier increases slightly in the new parameters over the tundra area of Canada and Russia, and the Tibet plateau.

3.6 Surface climate over western US

A one-year simulation is not long enough to allow CLM to be spun up to simulate realistic land surface conditions for the simulation period. Nevertheless, to demonstrate how high-resolution surface parameters could be used to support regional climate modeling, simulated surface albedo and surface fluxes are plotted to provide some indications of the impacts of grid resolution in simulating land-atmosphere interactions. Figure 11 shows the simulated surface albedo and sensible and latent heat fluxes for the summer (June-July-August) after eight months of simulation. Spatial variability of surface albedo shows important features arising from mountain snowpack over the Central and Northern Rocky Mountain and at the higher latitudes. Surface albedo is generally rather uniform elsewhere, but lower albedo values corresponding to the forest along the Coastal Range, Cascades, and Sierra Nevada of Washington and California are clearly shown, as well as higher albedo values corresponding to the bare soil seen in the high resolution data displayed in Fig. 4a. Sensible and latent heat fluxes are dominated by spatial variability associated with topography and mountain snowpack. Nevertheless, some spatial variability can be identified that corresponds with fine spatial features of vegetation that influence sensible and latent heat fluxes, e.g., lower Bowen ratio at North Dakota, South Dakota, Nebraska, Kansas, Oklahoma where grass were dominated (Fig. 11d). However, we also noted some jagged patterns in the latent heat flux (e.g., in western Montana) due to the coarse resolution soil texture data used in the simulation. This shows the sensitivity of surface heat fluxes to different surface parameters and highlights the importance of developing a consistent high-resolution dataset for all the vegetation and soil parameters for high-resolution land surface modeling.

4 Discussion

A new set of CLM land surface parameters has been generated consistently from the latest version of MODIS land cover product (MCD12Q1 C5) and an improved MODIS LAI product in the year 2005. The MCD12Q1 C5 has been evaluated systematically and demonstrated to have an overall accuracy of over 75 % (Friedl et al., 2010), meaning that on average 75 % of the land area were correctly classified, while the data sources of the current CLM 4.0 parameters have varying degrees of quality, with some having no quality assessment. For example, MODIS VCF product did not have sufficient validation of bare soil/herbaceous coverage and the existing validations of tree cover data

Title Page
Abstract Introduction
Conclusions References
Tables Figures
◀| |▶
◀ ▶
Back Close
Full Screen / Esc
Printer-friendly Version
Interactive Discussion

reported various qualities across biomes (Hassen et al., 2003; Montesano et al., 2009; White et al., 2005; Jeganathan et al., 2009). Furthermore, the current CLM 4.0 parameters were derived from various datasets spanning 1991 to 2008. Due to the higher resolution of the source data, the new parameters have been derived for a resolution of 0.05°, while the current CLM 4.0 parameters have much coarser resolution of 0.5°. Our analysis also shows that the new parameters could resolve more PFTs within each grid due to the higher resolution of the MCD12Q1 C5 product. The high-resolution new parameters enable model simulation at finer model grids than typical CLM simulations performed in the past, and thus enable regional analysis of land surface processes and their impacts on climate variability and change.

For vegetated surfaces, the new parameters produced much different global distribution of PFTs compared to the CLM 4.0 parameters, with the largest decrease in bare soil and increase in shrub coverage. Evaluation over CONUS shows that the shrub lands and bare soil estimated by new parameters are more accurate when NLCD is used as reference. This could be partially attributed to different land cover representations in land cover classification product and vegetation continuous field product. Both MCD12Q1 and NLCD data classified pixels (500 m in MCD12Q1 and 30m in NLCD) into dominant land cover types (e.g., NLCD defined “barren land” as area that has at least 85 % non-vegetated coverage), while MODIS VCF estimated the composition of bare soil, trees, and herbaceous within each pixel. Although the MODIS VCF seems to be able to produce more realistic estimation of the fraction of each PFT within grid cells, the bare soil fraction has not been validated. Previous study showed that VCF underestimate tree cover, i.e., overestimate the bare ground in south western US (White et al., 2005). This is consistent with our findings using NLCD. Our evaluation shows that the MODIS VCF has considerable overestimation of bare soil, even if only land with over 85 % of bare soil is considered (3.5 % compared to 2.0 % in Table 3).

The new parameters decrease Needleleaf Evergreen trees and increase Needleleaf Deciduous trees over all land. This pattern is mainly found in the boreal region. Interestingly, in the Amazon region the current CLM 4.0 parameters reported no Needleleaf trees while the new parameters have some coverage (0.1–0.4 %) in the Andes Mountains and Brazilian Shield. This confirms that the new parameters have capability of resolving more PFTs within each $0.5^\circ \times 0.5^\circ$ grid cell.

The new parameters have slightly increased coverage of Broadleaf Evergreen trees over all land. This change is largely caused by the difference in MCD12Q1 land cover used by the new parameters and the AVHRR continuous fields data that was used for disaggregating the fraction of trees into Needleleaf and Broadleaf, as well as Evergreen and Deciduous component.

The new parameters have considerable decrease in Broadleaf Deciduous trees over all land. The largest decrease is found in the Amazon region, where the decrease is replaced by the increase in shrub and grass percentage in Brazil Shield. The new parameters have decreased the percentage of Broadleaf Deciduous Boreal trees but slightly increased Broadleaf Deciduous Temperate trees. This can be caused by the differences and increased resolution in climate data, i.e., WorldClim (Hijmans et al., 2005) compared to Willmott and Matsuura Climate (Willmott and Matsuura, 1999) used to generate CLM 4.0 parameters.

For global grass PFTs, the new parameters have overall increased estimation, with decreased coverage of C3 grass and increased coverage of C4 grass. This pattern can be found clearly in the Amazon region and Sahara & Arabia Region, which can be caused by increased representation of grass in MCD12Q1 compared to the MODIS VCF product and the difference in climate data used for the two sets of parameters.

Overall, in the new parameters the global land had decreased contribution from bare soil and tree PFTs, but increased contribution from shrub, grass and crop. This pattern is also found over CONUS. Evaluation using finer resolution NLCD over CONUS shows that the new parameters produce more accurate estimation of bare soil, grass and shrub land coverage when compared to NLCD. However, as aforementioned it can also be explained by the fact that the MCD12Q1 data and NLCD are both discrete land cover classification and have similar definition of the classes. For grass land, the new parameters generate less accurate spatial representation. The dominant grass areas

Title Page
Abstract Introduction
Conclusions References
Tables Figures
◀| |▶
◀ ▶
Back Close
Full Screen / Esc
Printer-friendly Version
Interactive Discussion

in the western US are represented as a mixture of trees, shrubs and grass in NLCD, which reveals the potential problem of using discrete classification scheme. Although studies existed to partition the land cover classes in MCD12Q1 into mixture of PFTs, the composition of each PFTs in the grids are usually assigned artificially (Poulter et al., 2011).

Both new and CLM 4.0 parameters have large increase of cropland compared to NLCD. However, it seems that NLCD tends to underestimate US crop land area. If compared with USDA NASS statistics, the new parameters have significant overestimation of crop land. The overestimation is mainly distributed over Midwest US, where both CLM 4.0 and NLCD show considerable percentage of grass. This indicates that MCD12Q1 might have poor performance in identifying crop from grass.

The new parameters have an overall decrease of combined LAI for all seasons and large discrepancy in spatial distribution of combined LAI compared to the CLM 4.0 parameters, especially in tropical and boreal regions. In tropical region, the new parameters produce substantially higher LAI values for all seasons, while in high latitude Northern Hemisphere the new parameters have substantially lower LAI values. This reflects the large change made in the improved LAI product compared to the original MODIS LAI product (MOD15A2 C4) used by CLM 4.0 parameters. First, the improved LAI product is based on the latest release of MODIS LAI (MOD15A2 C5) rather than MOD15A2 C4 which has overestimation in global LAI reported by many studies (Fang and Liang, 2005, Garrigues et al., 2008, Lacaze et al., 2008, Hill et al., 2006, Pisek and Chen, 2007 and Weiss et al., 2007). Second, the PFT LAI in CLM 4.0 parameters is calculated from the three-year monthly mean LAI. Yuan et al. (2011) pointed out that the multi-year mean monthly LAI tend to underestimate the real LAI value in the tropical region because of the large fluctuation of LAI time-series due to frequent cloud cover. The improved LAI product used the latest release of MODIS LAI (MOD15A2 C5) that adopted temporal spatial filter to avoid this problem and yielded more accurate LAI estimation validated using observation data. However, MOD15A2 C5 was reported to have underestimation of needleleaf LAI (De Kauwe et al., 2011), which explained that the new parameters have decreased combined LAI in the Northern Hemisphere boreal region. Since the combined LAI analysis is also influenced by the PFT fraction, the increased broadleaf trees in the tropical forest and decreased Needleleaf trees in the boreal region also contributed to the higher combined LAI in tropical and lower LAI in boreal region.

The new parameters have generally good agreement with MODIS JJA LAI globally except for some temperate and tropical regions. The differences can be attributed to the adjustment of maximum and minimum PFT LAI based on the method in Bonan et al. (2002). Likewise, the increase of tropical and boreal LAI in tropical and boreal region during DJF, MAM, and SON seasons may also have resulted from the adjustment for Evergreen trees LAI, which confines the lower limit of LAI to be the fraction of maximum monthly LAI. This also indicates that MODIS LAI data need to be improved in the higher latitude area to alleviate the underestimation of LAI caused by snow contamination in cold seasons.

The new parameters adopt the same method of SAI mapping as Lawrence and Chase (2007), which was based on the combination of PFT LAI and SAI phenology. Thus the differences between SAI in the new parameters and SAI in the CLM 4.0 parameters have similar spatial distribution as LAI differences.

The individual PFT LAI analysis shows the differences between the new parameters and CLM 4.0 parameters in terms of the LAI phenology cycle for each PFT. Overall, the new parameters have similar or lower average LAI for all PFTs in both northern and Southern Hemisphere except the Broadleaf Evergreen trees in Southern Hemisphere and Broadleaf Deciduous trees in both northern and Southern Hemisphere. In addition, the Broadleaf Deciduous Temperate and Boreal trees have greater LAI phenology fluctuation with higher maximum LAI and lower minimum LAI. In the Southern Hemisphere, the new parameters have better representation of phenology cycle, with LAI reaching maximum in austral summer and minimum in austral winter.

The new non-vegetated land cover parameters at 0.05° resolution were aggregated to 0.5° for comparison with the CLM 4.0 parameters. The new parameters produced slightly increased glacier coverage and substantially increased lake and wetland coverage. It is believed that the lake coverage estimated by the new parameters is more realistic since MCD12Q1 500 m product has over 95 % of accuracy in open water identification (Friedl et al., 2010) while the CLM 4.0 lake percentage is based on outdated freshwater map at resolution of 1°. There is a considerable decrease in urban area in the new parameters. This can be explained by the fact that the new urban parameter is based on MCD12Q1, which identifies buildings and man-made structures as urban area while the CLM 4.0 parameters used LandScan population data to estimate urban area.

The simulation of CLM using the new land surface parameters over western US showed finer scale features on top of the dominant topographic patterns corresponding to the high-resolution surface parameters. The global high-resolution parameters can be used in high-resolution offline and coupled modeling globally to support different scientific investigations or development of high-resolution data assimilation products.

5 Conclusions

In this study we developed high-resolution global land surface data for the Community Land Model that enables the model to simulate detailed land surface processes at regional scale. Compared to the current CLM 4.0 parameters, the new land surface parameters not only with have much higher resolution but they are also generated consistently from the latest MODIS land cover MCD12Q1 C5 and improved MODIS LAI product which have been systematically validated.

Our analysis shows that the new parameters generally identify more PFTs per grid than the current CLM 4.0 parameters due to the higher spatial resolution of MODIS land cover products. Over global land, the new parameters have decreased contribution from bare soil and trees, but increased contribution from grass, shrub and crop. The differences can be attributed to the change in source data and also partly to the discrete classification scheme used in MCD12Q1. Potential improvement can be made by estimating fraction of PFTs within each MCD12Q1 grid cell based on both dominant classes provided by MCD12Q1 and supporting remotely sensed data such as vegetation indices or vegetation vertical structure from Light Detection and Ranging (LiDAR) data.

Compared to the current CLM 4.0 parameters, the new parameters have increased LAI and SAI in tropical region while decreased LAI and SAI in boreal region. The combined LAI in the new parameters are close to the improved MODIS LAI in JJA, while higher than the observed LAI in the Northern Hemisphere boreal region during other seasons due to the adjustment for evergreen trees. This suggests that MODIS may be improved in the cold season to alleviate snow contamination.

The new parameters provide higher resolution non-vegetated land cover, and more realistic land water representation. Our regional climate simulation based on the new parameters over Western US show that the finer scale land surface datasets improve the resolution of model surface heat fluxes, which highlights the importance of developing high-resolution datasets for land surface modeling. Future work will include global tests of CLM in order to examine the impact of the land parameter change on simulated land surface processes.

Acknowledgements. Development of the high-resolution surface parameters and the WRF-CLM coupled simulation was supported by the Pacific Northwest National Laboratory (PNNL) Integrated Regional Earth System Modeling (iRESM) Initiative. Analysis and evaluation of the high-resolution surface parameters were supported as part of the efforts to develop a new subgrid classification scheme for CLM for the Climate Science for Sustainable Energy Future (CSSEF) Project funded by the Department of Energy Earth System Modeling Program. PNNL is operated by Battelle for the DOE under Contract DE-AC06-76RLO 1830.

References

Bonan, G. B., Levis, S., Kergoat, L., and Oleson, K. W.: Landscapes as patches of plant functional types: An integrating concept for climate and ecosystem models, Global Biogeochem. Cy., 16, doi:10.1029/2000GB001360, 2002a.

Bonan, G. B., Oleson, K. W., Vertenstein, M., Levis, S., Zeng, X., Dai, Y., Dickinson, R. E., and Yang, Z. L.: The land surface climatology of the Community Land Model coupled to the NCAR Community Climate Model. J. Climate, 15, 3123–3149, 2002b.

Cogley, J. G.: GGHYDRO – Global Hydrographic Data Release 2.0. Trent Climate Note 91-1, Dept. Geography, Trent University, Peterborough, Ontario, 1991.

De Kauwe, M. G., Disney, M. I., Quaif, T., Lewis, P., and Williams, M.: An assessment of the MODIS collection 5 leaf area index product for a region of mixed coniferous forest, Remote Sens. Environ., 115, 767–780, 2011.

Dickinson, R. E., Oleson, K. W., Bonan, G., Hoffman, F., Thornton, P., Vertenstein, M., Yang, Z. L., and Zeng, X.: The Community Land Model and its climate statistics as a component of the Community Climate System Model. J. Climate, 19, 2302–2324, 2006.

Fang, H. and Liang, S.: A hybrid inversion method for mapping leaf area index from MODIS data: Experiments and application to broadleaf and needleleaf canopies, Remote Sens. Environ., 94, 405–424, 2005.

Fang, H., Wei, S., and Liang, S.: Validation of MODIS and CYCLOPES LAI products using global field measurement data, Remote Sens. Environ., 119, 43–54, 2012.

Friedl, M. A., Sulla-Menashe, D., Tan, B., Schneider, A., Ramankutty, N., Sibley, A. and Huang, X.: MODIS Collection 5 Global Land Cover: Algorithm refinements and characterization of new datasets, Remote Sens. Environ., 114, 168–182, 2010.

Fry, J., Xian, G., Jin, S., Dewitz, J., Homer, C., Yang, L., Barnes, C., Herold, N., and Wickham, J.: Completion of the 2006 National Land Cover Database for the Conterminous United States, Photogramm. Eng. Remote Sens., 77, 858–864, 2011.

Garrigues, S., Lacaze, R., Baret, F., Morisette J. T., Weiss, M., Nickeson, J. E., Fernandes, R., Plummer, S., Shabanov, N. V., Myneni, R. B., Knyazikhin, Y., and Yang, W.: Validation and intercomparison of global Leaf Area Index products derived from remote sensing data. J. Geophys. Res., 113, G02028, doi:10.1029/2007JG000635, 2008.

Hansen, M. C., DeFries, R. S., Townshend, J. R. G., Carroll, M., Dimiceli, C., and Sohlberg, R. A.: Global Percent Tree Cover at a Spatial Resolution of 500 Meters: First Results of the MODIS Vegetation Continuous Fields Algorithm, Earth Interact., 7, 1–15, 2003.

Hijmans, R. J., Cameron, S. E., Parra, J. L., Jones, P. G., and Jarvis, A.: Very high resolution interpolated climate surfaces for global land areas. Int. J. Climatol., 25, 1965–1978, 2005.

Hill, M. J., Senarath, U., Lee, A., Zeppel, M., Nightingale, J. M., Williams, R. D. J., and McVicar, T. R.: Assessment of the MODIS LAI product for Australian ecosystems, Remote Sens. Environ., 101, 495–518, 2006.

Jeganathan, C., Dadhwal, V. K., Gupta, K., and Raju, P. L. N.: Comparison of MODIS vegetation continuous field – based forest density maps with IRS-LISS III derived maps, J. Indian Soc. Remote Sens., 37, 539–549, 2009.

Jin, J., Miller, N. L., and Schlegel, N.: Sensitivity Study of Four Land Surface Schemes in the WRF Model, Adv. Meteorol., doi:10.1155/2010/167436, 2010.

Lawrence, P. J. and Chase, T. N.: Representing a MODIS consistent land surface in the Community Land Model (CLM 3.0): Part 1. Generating MODIS consistent land surface parameters, Coop. Inst. for Res. Environ. Sci., Univ. of Colo., Boulder, 2006.

Lawrence, P. J. and Chase, T. N.: Representing a new MODIS consistent land surface in the Community Land Model (CLM 3.0), J. Geophys. Res., 112, G01023, doi:10.1029/2006JG000168, 2007.

Lawrence, D., Oleson, K. W., Flanner, M. G., Thorton, P. E., Swenson, S. C., Lawrence, P. J., Zeng, X., Yang, Z. L., Levis, S., and Skaguchi, K.: Parameterization improvements and functional and structural advances in version 4 of the Community Land Model, J. Adv. Model. Earth Syst., 3, M03001, doi:10.1029/2011MS000045, 2011.

Leung, L. R., Kuo, Y.-H., and Tribbia, J.: Research Needs and Directions of Regional Climate Modeling Using WRF and CCSM, B. Am. Meteorol. Soc., 87, 1747–1751, doi:10.1175/BAMS-87-12-1747, 2006.

Li, H., Huang, M., Wigmosta, M. S., Ke, Y., Coleman, A. M., Leung, L. R., Wang, A., and Ricciuto, D. M.: Evaluating runoff simulations from the Community Land Model 4.0 using observations from flux towers and a mountainous watershed, J. Geophys. Res., 116, D24120, doi:10.1029/2011JD016276, 2011.

Loveland, T. R. and Belward, A. S.: The IGBP-DIS global 1 km land cover data set, DISCover: First results, Int. J. Remote Sens., 18, 3291–3295, 1997.

Maslowski, W., Cassano, J., Gutowski, W., and Lettenmaier, D.: Regional Arctic Climate System Model (RACM) – Development and Selected Results. Geophysical Research Abstracts, 13, EGU2011-9648, EGU General Assembly 2011, 2011.

Montesano, P. M., Nelson, R., Sun, G., Margolis, H., Kerber, A., and Ranson, K. J.: MODIS tree cover validation for the circumpolar taiga–tundra transition zone, Remote Sens. Environ., 113, 2130–2141, 2009.

Oleson, K. W., Lawrence, D. M., Bonan, G. B., Flanner, M. G., Kluzek, E., Lawrence, P. J., Levis, S., Swenson, S. C., Thornton, P. E., Dai, A., Decker, M., Dickinson, R., Feddema, J., Heald, C.L., Hoffman, F., Lamarque, J.-F., Mahowald, N., Niu, G.-Y., Qian, T., Randerson, J., Running, S., Sakaguchi, K., Slater, A., Stockli, R., Wang, A., Yang, Z.-L., Zeng, X., and Zeng, X.: Technical Description of version 4.0 of the Community Land Model (CLM), NCAR/TN-478+STR, www.cesm.ucar.edu/models/ccsm4.0/clm/CLM4_Tech_Note.pdf, 2010.

Pisek, J. and Chen, J. M.: Comparison and validation of MODIS and VEGETATION global LAI products over four BigFoot sites in North America, Remote Sens. Environ., 109, 81–94, 2007.

Poulter, B., Ciais, P., Hodson, E., Lischke, H., Maignan, F., Plummer, S., and Zimmermann, N. E.: Plant functional type mapping for earth system models, Geosci. Model Dev., 4, 993–1010, doi:10.5194/gmd-4-993-2011, 2011.

Skamarock, W. C., Klemp, J. B., Dudhia, J., Gill, D. O., Barker, D. M., Duda, M. G., Huang, X.Y., Wang, W., and Powers, J. G.: A Description of the Advanced Research WRF Version 3, NCAR Technical Note, NCAR/TN–475+STR, 123 pp., 2008.

Still, C. J., Berry, J. A., Collatz, G. J., and DeFries, R. S.: Global distribution of C3 and C4 vegetation: Carbon cycle implications, Global Biogeochem. Cy., 17, 1006–1019, 2003.

Subin, Z. M., Riley, W. J., Jin, J., Christianson, D. S., Torn, M. S., and Kueppers, L. M.: Ecosystem Feedbacks to Climate Change in California: Development, Testing, and Analysis Using a Coupled Regional Atmosphere and Land Surface Model (WRF3-CLM3.5), Earth Interact., 15, 1–38, 2011.

Weiss, M., Baret, F., Garrigues, S., and Lacaze, R.: LAI and fPAR CYCLOPES global products derived from VEGETATION. Part 2: Validation and comparison with MODIS collection 4 products, Remote Sens. Environ., 110, 317–331, 2007.

Willmott, C. J. and Matsuura, K.: Terrestrial air temperature and precipitation: Monthly and annual climatologies (Version 2.0.1), http://climate.geog.udel.edu/~climate/html_pages/download.html, 2000.

White, M. A., Shaw, J. D., and Ramsey, R. D.: Accuracy assessment of the vegetation continuous field tree cover product using 3954 ground plots in the southwestern USA, Int. J. Remote Sens., 26, 2699–2704, 2005.

Yuan, H., Dai, Y., Xiao, Z., Ji, D., and Shangguan, W.: Reprocessing the MODIS Leaf Area Index products for land surface and climate modeling, Remote Sens. Environ., 115, 1171–1187, 2011.

Table 1. Properties of new and CLM 4.0 land surface data.

Surface data	Resolution		Source data		Source date	
	New	CLM 4.0	New	CLM 4.0	New	CLM 4.0
Glacier	0.05°	0.5°	MCD12Q1 PFT classification	IGBP DISCover	2005	2000
Lake	0.05°	0.5°	MCD12Q1 PFT classification, ESRI landmass boundaries	1° by 1° global perennial freshwater lakes and swamps/marshes	2005	1991
Wetland	0.05°	0.5°	MCD12Q1 IGBP classification	1° by 1° global perennial freshwater lakes and swamps/marshes	2005	1991
Urban	0.05°	0.5°	MCD12Q1 PFT classification	LandScan population density dataset	2005	2004
PFTs	0.05°	0.5°	MCD12Q1 PFT classification, WorldClim climate	AVHRR continuous fields , MODIS vegetation continuous fields Willmott and Matsuura Climate, global agriculture land based on Ramankutty, 2008	2005	Mixed years from 1993 to 2008
LAI and SAI	0.05°	0.5°	Continuous LAI improved from MOD15A1	MCD15A2	2005	2001–2003

Table 2. Reclassification of new, CLM4.0 PFT parameters and NLCD land cover classes.

CLM PFTs	NLCD Land-Cover Classes	Generalized land cover classes
Needleleaf Evergreen Temperate trees; Needleleaf Evergreen Boreal trees; Needleleaf Deciduous Boreal trees; Broadleaf Evergreen Tropical trees; Braodleaf Evergreen Temperate trees; Broadleaf Deciduous Tropical trees; Broadleaf Deciduous Boreal trees	Evergreen forest; Deciduous forest; Mixed forest; Woody wetland	Tree
Broadleaf Evergreen Temperate shrubs; Braodleaf Deciduous Temperate shrubs; Broadleaf Deciduous Boreal shrubs	Dwarf Scrub; Shrub/Scrub	Shrub
C3 Arctic grass; C3 non-Arctic grass, C4 grass	Grassland/Herbaceous; Pasture/Hay; Developed, open space; Developed, low intensity; Herbaceous wetland	Grass
Crop	Cultivated crops	Crop
Bare soil excluding open water in CLM surface parameter	Barren land; Developed, medium Intensity; Developed, high intensity; Perrennial Ice/Snow	Bare ground

Table 3. Average global and regional PFT composition[a].

PFT	All land		Amazon		Boreal		Sahara & Arabia	
	CLM 4.0	New (Diff)	CLM 4.0	New (Diff)	CLM 4.0	New (Diff)	CLM 4.0	New (Diff)
Bare	33.5	24.7 (−9.2)	3.8	2.4 (−1.4)	12.0	6.1 (−5.9)	87.8	78.3 (−9.5)
Ndl Evg Tmp	3.0	2.2 (−0.8)	0.0	0.4 (+0.4)	2.7	4.0 (+1.3)	0.1	0.0 (–)
Ndl Evg Borl	6.4	5.2 (-1.2)	0.0	0.2 (+0.2)	29.0	21.0 (−8.0)	0.0	0.0 (–)
Ndl Dec Borl	1.0	2.3 (+1.3)	0.0	0.1 (+0.1)	4.9	10.6 (+5.8)	0.0	0.0 (–)
Brd Evg Trop	8.7	9.4 (+0.7)	49.8	52.3 (+2.5)	0.0	0.0 (–)	0.0	0.0 (–)
Brd Evg Tmp	1.4	1.6 (+0.2)	1.7	1.1 (−0.6)	0.0	0.4 (+0.4)	0.0	0.0 (–)
Brd Dec Trop	5.1	2.8 (−2.3)	14.4	5.8 (−8.6)	0.0	0.0 (–)	0.4	0.4 (–)
Brd Dec Tmp	3.3	2.5 (−0.8)	0.2	0.1 (−0.1)	1.7	1.8 (+0.1)	0.0	0.0 (–)
Brd Dec Borl	1.2	0.9 (−0.3)	0.0	0.0 (–)	3.9	2.4 (−1.5)	0.0	0.0 (–)
Shr Evg Tmp	0.1	0.7 (+0.6)	0.0	0.1 (+0.1)	0.0	0.3 (+0.3)	0.0	0.6 (+0.6)
Shr Dec Tmp	3.8	11.2 (+7.4)	2.3	6.5 (+4.2)	0.1	0.3 (+0.2)	1.7	9.9 (+8.2)
Shr Dec Borl	5.4	6.7 (+1.3)	1.0	0.5 (−0.5)	24.0	39.3 (+15.3)	0.0	0.0 (–)
Grs C3 Arctic	2.9	3.1 (+0.2)	0.6	0.8 (+0.2)	9.9	9.1 (−0.8)	0.0	0.0 (–)
Grs C3	8.2	6.7 (−1.5)	5.9	3.0 (−2.9)	4.8	4.1 (−0.7)	1.2	0.4 (−0.8)
Grs C4	7.5	8.6 (+1.1)	17.1	22.1 (+4.4)	0.0	0.1 (+0.1)	5.8	8.6 (+3.8)
Crop	8.5	11.1 (+2.6)	3.0	4.5 (+1.5)	7.0	10.2 (+3.2)	2.9	1.8 (−1.1)

[a] Differences between new parameters and CLM 4.0 parameters are shown in brackets, with a dash indicating no change. Abbreviation: Ndl Evg Tmp = Needleleaf Evergreen Temperate trees; Ndl Evg Borl = Needleleaf Evergreen Boreal trees; Ndl Dec Borl = Needleleaf Deciduous Boreal trees; Brd Evg Trop=Broadleaf Evergreen Tropical trees; Brd Evg Tmp=Broadleaf Evergreen Temperate trees; Brd Dec Trop = Broadleaf Deciduous Tropical trees; Brd Dec Tmp=Broadleaf Deciduous Temperate trees; Brd Dec Borl = Broadleaf Deciduous Boreal trees; Shr Evg Tmp = Broadleaf Evergreen Temperate shrubs; Shr Dec Tmp = Broadleaf Deciduous Temperate shrubs; Shr Dec Borl = Broadleaf Deciduous Boreal shrubs; Grs C3 Arctic = C3 Arctic grass; Grs C3 = C3 non-Arctic grass; Grs C4 = C4 grass.

Table 4. Percentage of land cover types for new, CLM4 and reference data over CONUS.

Data	Trees	Shrub	grassland	Cropland	Bare soil
CLM 4.0	31.5	4.8	25.1	20.5	14.8 Over 85 % of bare soil: 3.5
New	25.2	14.8	28.3	25.0	2.7
NLCD	28.8	21.4	28.5	15.5	2.0
USDA NASS	NA	NA	NA	Year 2007: 20.3 Year 2002: 21.7	NA

Table 5. Average global and regional seasonal LAI and SAI for new and CLM 4.0 parameters.

Season	Global		Boreal		Amazon		Sahara	
	CLM 4.0	New (Diff)	CLM 4.0	New	CLM 4.0	New	CLM 4.0	New
LAI								
DJF	0.68	0.60 (−0.08)	0.75	0.52 (−0.23)	3.02	3.33 (+0.31)	0.06	0.05 (−0.01)
MAM	0.92	0.80 (−0.12)	1.34	1.10 (−0.25)	3.22	3.38 (+0.16)	0.05	0.06 (+0.01)
JJA	1.09	0.93 (−0.15)	1.97	1.46 (−0.51)	3.09	3.49 (+0.40)	0.10	0.12 (+0.02)
SON	0.73	0.63 (−0.10)	0.83	0.61 (−0.22)	2.99	3.27 (+0.28)	0.08	0.07 (−0.01)
SAI								
DJF	0.28	0.22 (−0.06)	0.52	0.40 (−0.12)	0.70	0.69 (−0.01)	0.03	0.03 (+0.01)
MAM	0.29	0.24 (−0.05)	0.52	0.39 (−0.13)	0.70	0.72 (+0.02)	0.03	0.04 (+0.01)
JJA	0.33	0.29 (−0.04)	0.71	0.64 (−0.07)	0.72	0.70 (−0.02)	0.03	0.04 (+0.01)
SON	0.39	0.30 (−0.09)	0.80	0.55 (−0.25)	0.70	0.75 (+0.05)	0.05	0.06 (+0.01)

Table 6. Average global non−vegetated land cover composition.

Land Cover	CLM 4.0	New	Diff
Lake	0.52	1.4	0.88
Wetland	0.25	1.0	0.75
Urban	0.64	0.44	−0.2
Glacier	10.4	10.6	0.2

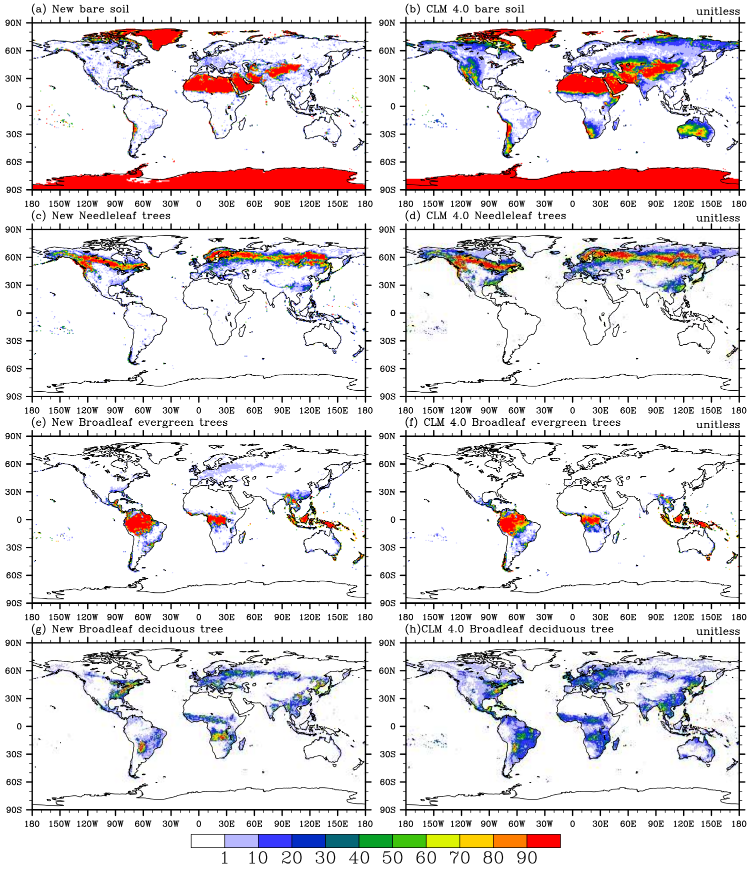

Fig. 1. Global distribution of bare soil, needleleaf trees, broadleaf evergreen trees and broadleaf deciduous trees for new and CLM 4.0 PFT parameters.

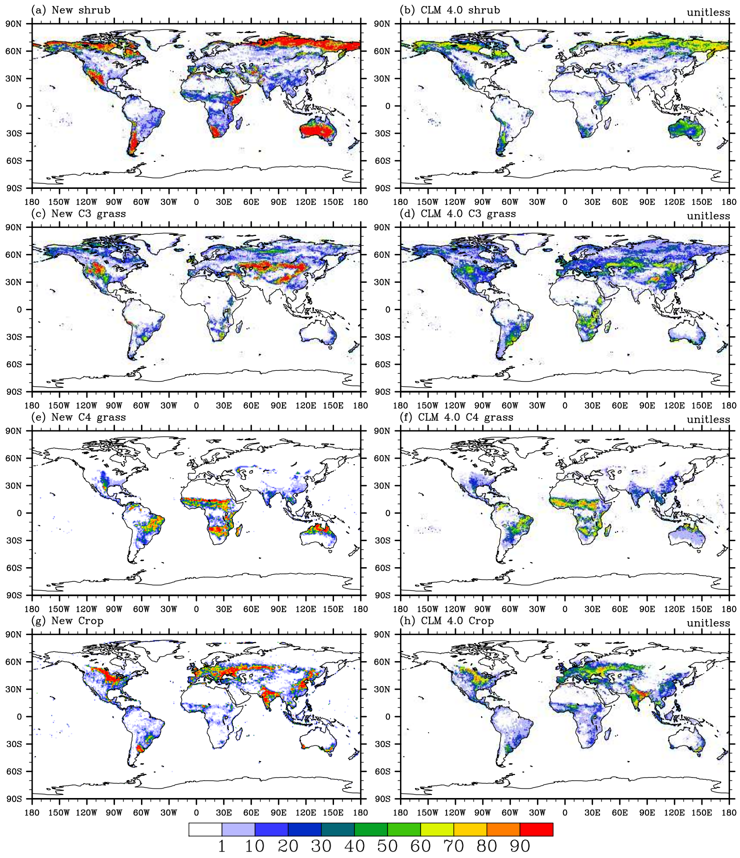

Fig. 2. Global distribution of shrub, C3 grass, C4 grass and crop for new and CLM 4.0 PFT parameters.

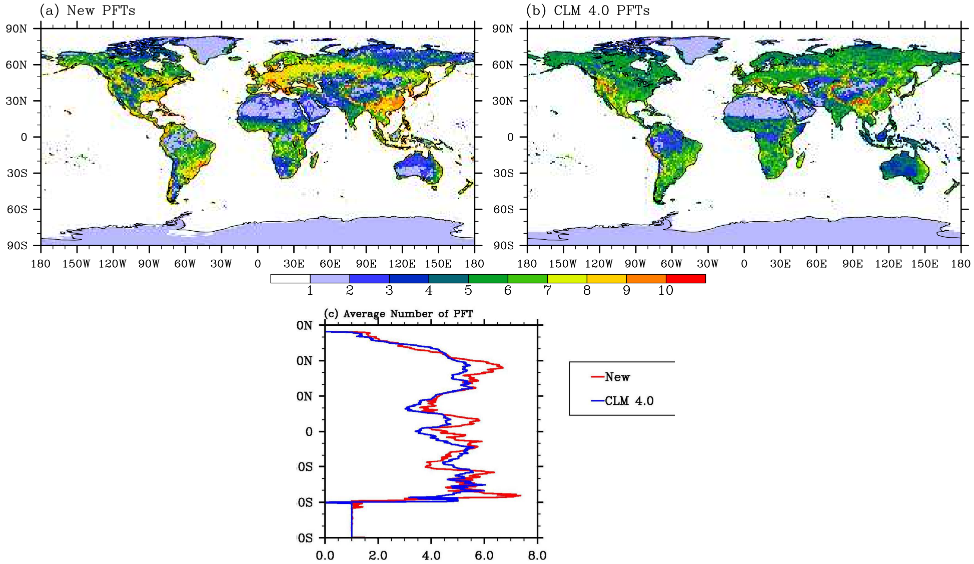

Fig. 3. (a) and **(b)**: Global distribution of number of PFTs; **(c)** Latitude distribution of average number of PFTs.

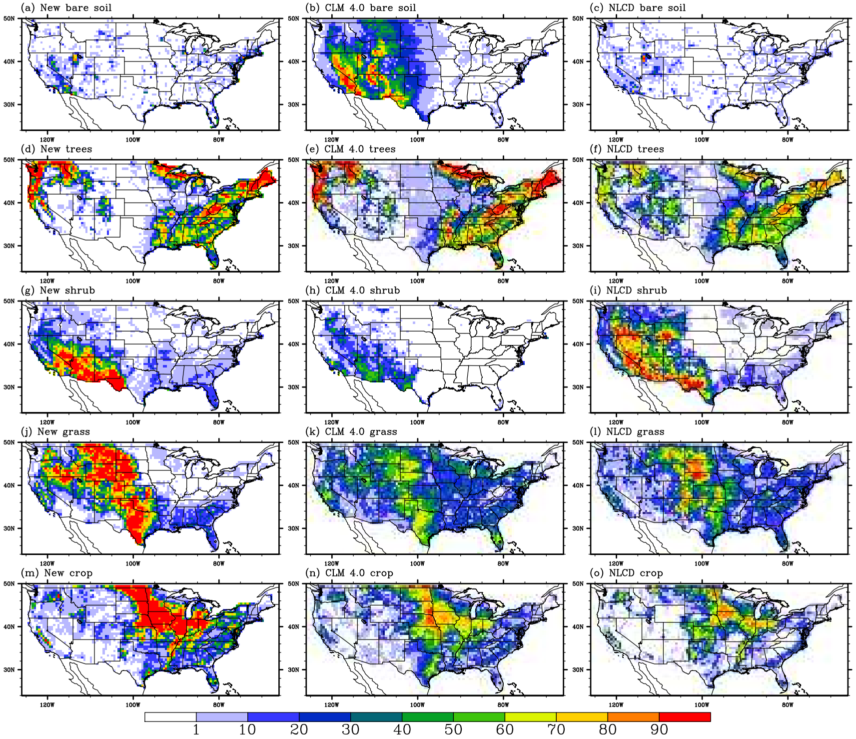

Fig. 4. Distribution of bare soil, shrub, grassland and crop over CONUS for new parameters, CLM 4.0 parameters and NLCD.

Title Page
Abstract
Introduction
Conclusions
References
Tables
Figures
◂◂
▸▸
◂
▸
Back
Close
Full Screen / Esc
Printer-friendly Version
Interactive Discussion

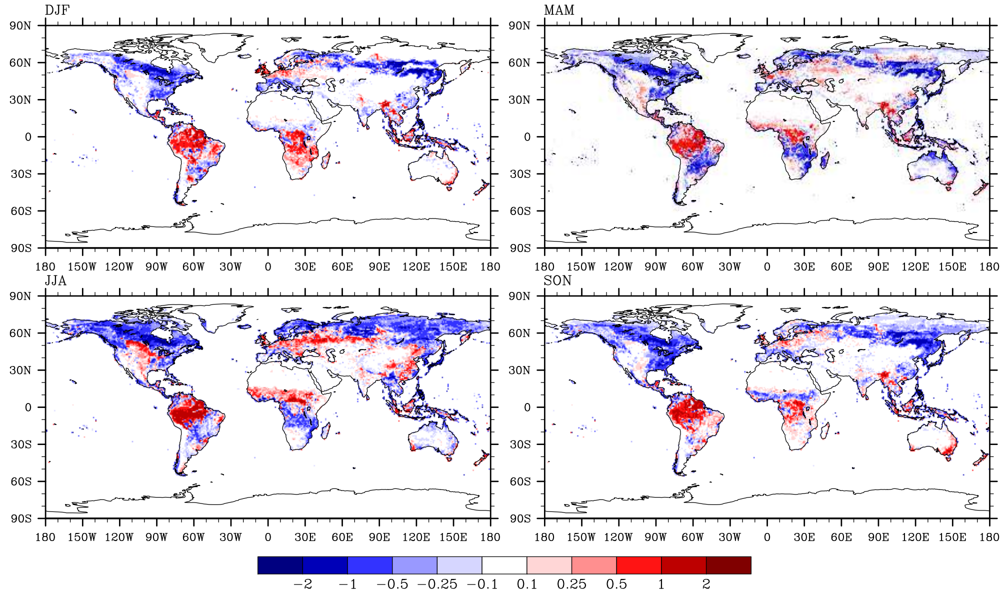

Fig. 5. Differences in seasonal LAI between new and CLM 4.0 parameters.

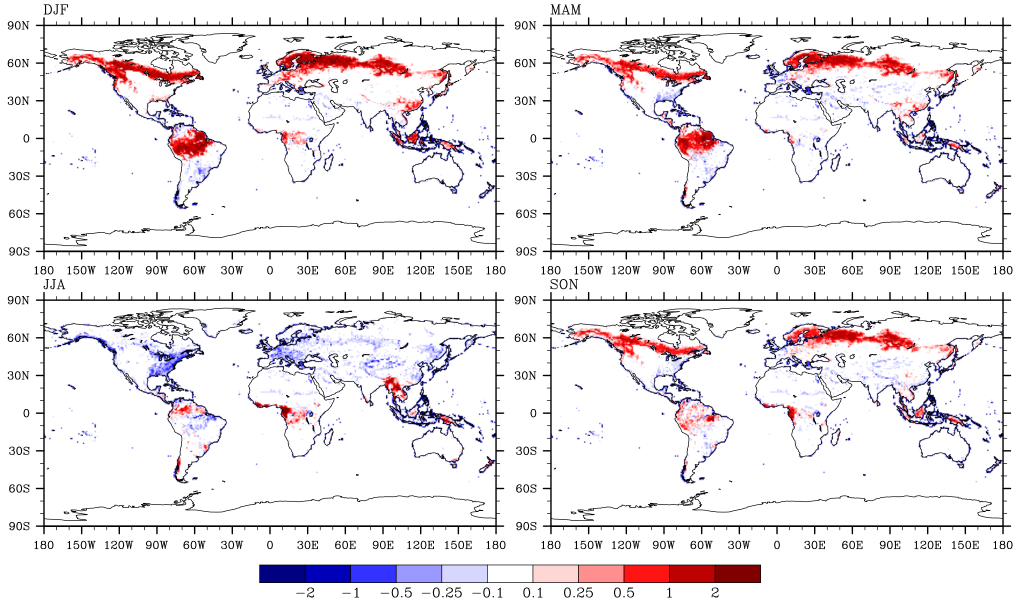

Fig. 6. Differences between new CLM LAI parameters and MODIS observed spatially and temporal improved LAI.

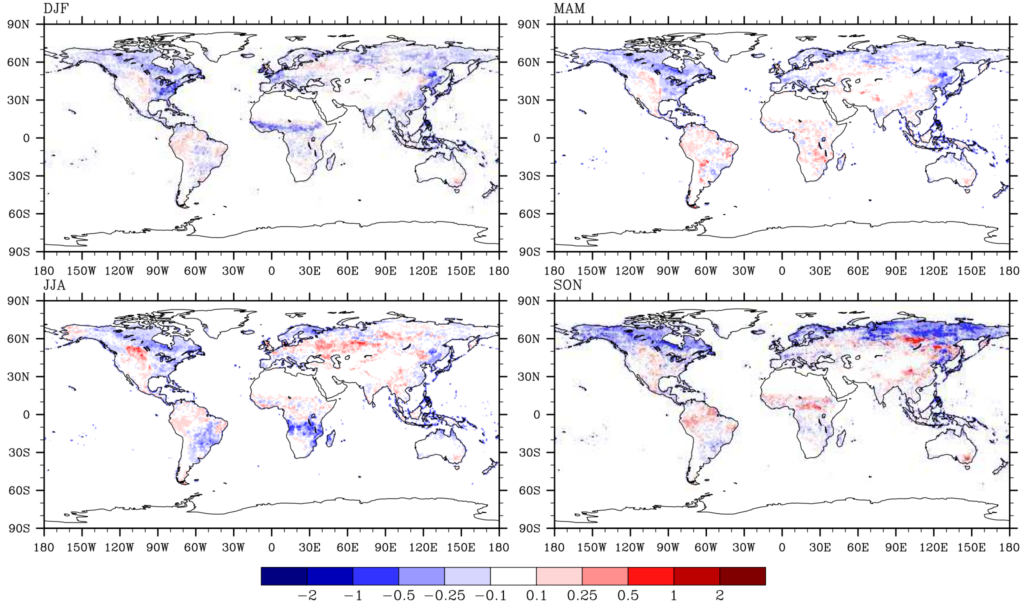

Fig. 7. Differences in seasonal SAI between new and CLM 4.0 parameters.

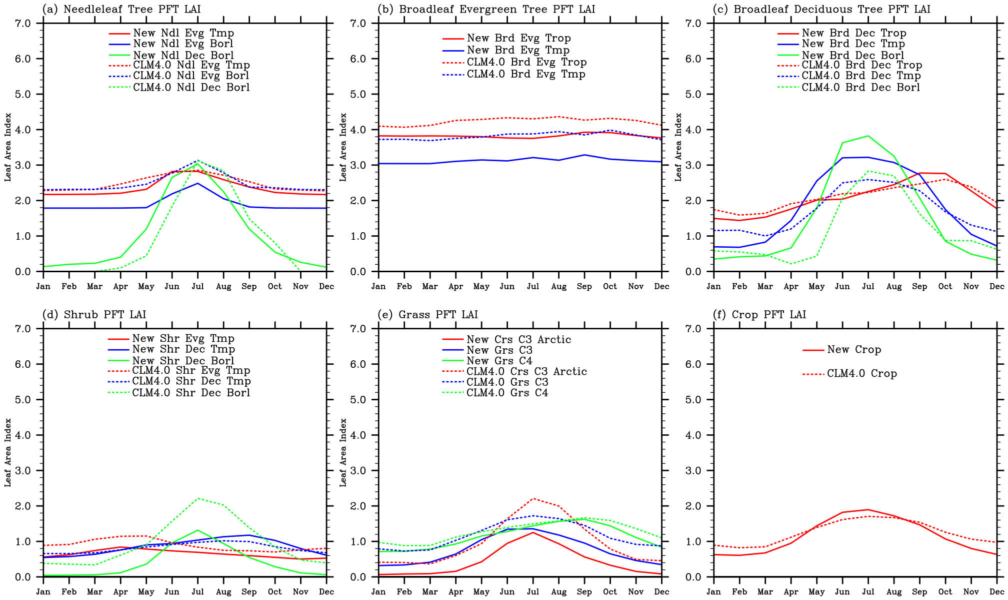

Fig. 8. Northern Hemisphere PFT LAI for new and CLM 4.0 parameters. The abbreviations of PFTs are same as in Table 3.

Title Page
Abstract | Introduction
Conclusions | References
Tables | Figures
◀ | ▶
◀ | ▶
Back | Close
Full Screen / Esc
Printer-friendly Version
Interactive Discussion

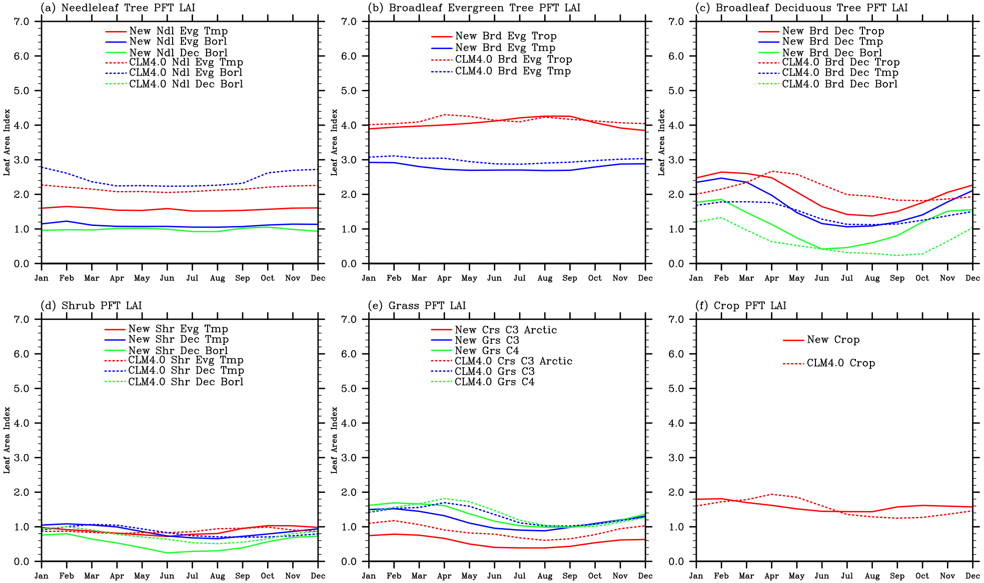

Fig. 9. Southern Hemisphere PFT LAI for new and CLM 4.0 parameters. The abbreviations of PFTs are same as in Table 3.

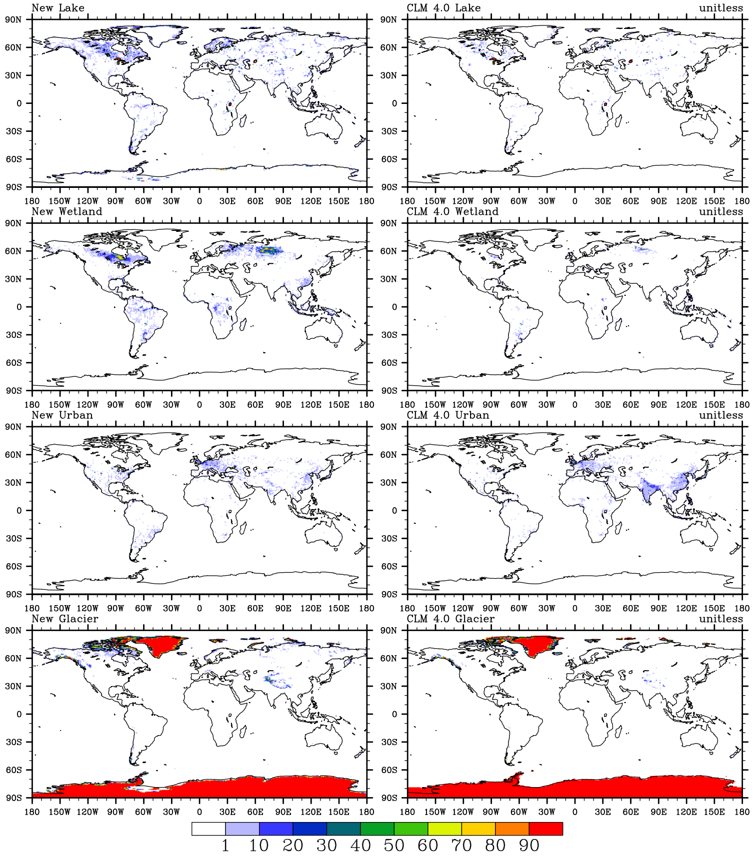

Fig. 10. Global distribution of non-vegetated land cover for new and CLM 4.0 parameters.

Title Page
Abstract
Introduction
Conclusions
References
Tables
Figures
◀|
|▶
◀
▶
Back
Close
Full Screen / Esc
Printer-friendly Version
Interactive Discussion

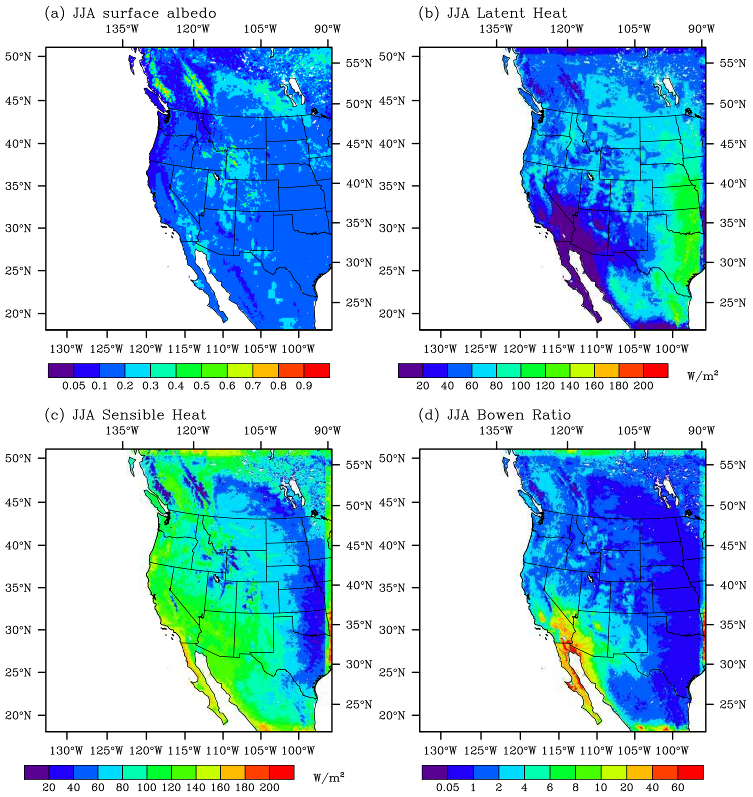

(a) JJA surface albedo

(b) JJA Latent Heat

(c) JJA Sensible Heat

(d) JJA Bowen Ratio

Fig. 11. Model simulated surface variables over western US using new parameters. **(a)** Surface temperature. **(b)** Sensible heat. **(c)** Latent heat. **(d)** Bowen ratio.